



HAL
open science

Homoepitaxial growth of device-grade GaAs using low-pressure remote plasma CVD

Lise Watrin, François Silva, Ludovic Largeau, Nathaniel Findling, Mirella Al Katrib, Muriel Bouttemy, Kassioyé Dembélé, Nicolas Vaissière, Cyril Jadaud, Pavel Bulkin, et al.

► **To cite this version:**

Lise Watrin, François Silva, Ludovic Largeau, Nathaniel Findling, Mirella Al Katrib, et al.. Homoepitaxial growth of device-grade GaAs using low-pressure remote plasma CVD. *Materials Science in Semiconductor Processing*, 2025, 186, pp.109069. <10.1016/j.mssp.2024.109069>. <hal-04814334>

HAL Id: hal-04814334

<https://hal.science/hal-04814334v1>

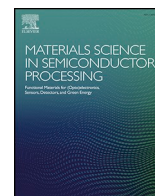
Submitted on 27 May 2025

HAL is a multi-disciplinary open access archive for the deposit and dissemination of scientific research documents, whether they are published or not. The documents may come from teaching and research institutions in France or abroad, or from public or private research centers.

L'archive ouverte pluridisciplinaire **HAL**, est destinée au dépôt et à la diffusion de documents scientifiques de niveau recherche, publiés ou non, émanant des établissements d'enseignement et de recherche français ou étrangers, des laboratoires publics ou privés.



Distributed under a Creative Commons CC BY 4.0 - Attribution - International License



Homoepitaxial growth of device-grade GaAs using low-pressure remote plasma CVD

Lise Watrin^{a,b}, François Silva^b, Ludovic Largeau^c, Nathaniel Findling^c, Mirella Al Katrib^{a,d}, Muriel Bouttemy^{a,d}, Kassioyé Dembélé^b, Nicolas Vaissière^e, Cyril Jadaud^b, Pavel Bulkin^b, Jean-Charles Vanel^b, Erik V. Johnson^b, Karim Ouaras^b, Pere Roca i Cabarrocas^{a,b,*}

^a Institut Photovoltaïque d'Ile-de-France (IPVF), 18 Boulevard Thomas Gobert, 91120, Palaiseau, France

^b LPICM, CNRS, École Polytechnique, Institut Polytechnique de Paris, route de Saclay, 91120, Palaiseau, France

^c C2N-CNRS/Université Paris-Sud – Université Paris-Saclay, 10 Boulevard Thomas Gobert, 91120, Palaiseau, France

^d Institut Lavoisier de Versailles (ILV), Université de Versailles Saint-Quentin-en-Yvelines, Université Paris-Saclay, CNRS, UMR 8180, 45 avenue des États-Unis, 78035, Versailles, France

^e III-V Lab, A Joint Lab of Nokia Bell Labs, Thales Research and Technology and CEA LETI, 91120 Palaiseau, France

ABSTRACT

We have achieved the growth of high-quality, homoepitaxial 100 GaAs thin films at 0.5 mbar and 500 °C using a Remote Plasma Chemical Vapor Deposition (RP-CVD) reactor. With this process, we demonstrate a film growth rate up to 3 μm/h, comparable to the conventional MOCVD technique. The resulting films exhibit structural characteristics close to those of commercial GaAs wafers, with excellent crystalline quality as confirmed by SAED patterns and XRD rocking-curve measurements for the 004 peak with a FWHM of 0.004°. AFM measurements reveal a surface roughness of 0.2 nm, similar to that of a polished wafer. Analysis of the chemical composition – as determined through XPS surface and depth-profiled measurements – indicates that the film is homogeneous, with a constant III/V ratio of 1 throughout the whole layer, and has no detectable carbon or oxygen contamination. Additionally, the films demonstrate a sharp photoluminescence peak (FWHM of 55 meV), a p-type doping concentration of 1.10¹⁸ cm⁻³, and a hole mobility of 172 cm² V⁻¹.s⁻¹. This work thus demonstrates a cost-effective growth method for III-V devices, enabled by the reduced gas consumption (only a few sccm, compared to tens of L/min in MOCVD) in RP-CVD operation at low pressure.

Gallium arsenide (GaAs) is a prominent III-V semiconductor material renowned for its superior electronic and optoelectronic properties [1]. With a direct bandgap of 1.43 eV at room temperature, GaAs offers high electron mobility, a high saturation velocity, and an excellent frequency response, making it an ideal candidate for high-speed and high-frequency applications [2]. These properties have led to its extensive use in a variety of devices, including light-emitting diodes (LEDs), high-electron-mobility transistors (HEMTs) and solar cells [3–5]. In the realm of photovoltaics, GaAs stands out as a leading material for III-V solar cells, offering exceptional efficiency, high radiation-hardness and reliability [6]. Indeed, thanks to its direct bandgap and superior electronic properties, GaAs solar cells achieve higher efficiency compared to silicon-based cells, especially under concentrated sunlight (current record at 30.8 % under 61 suns held by NREL [7]). However, the high cost of GaAs solar cells has been a significant barrier to their widespread adoption [8]. Reducing production costs while maintaining high quality is critical for expanding the use of GaAs in a wider range of PV applications. Therefore, exploring

cost-effective deposition techniques is of paramount importance.

Traditionally, the most commonly used techniques for depositing thin films of GaAs are metal-organic chemical vapor deposition (MOCVD) and molecular beam epitaxy (MBE) [9]. However, MOCVD and MBE have drawbacks, namely high cost and complex processes involving high-pressure (~500 mbar) or ultra-high vacuum conditions, respectively [10]. Plasma-assisted growth techniques, such as plasma-enhanced chemical vapor deposition (PECVD), provide a more economical method by using a plasma discharge to dissociate precursors at moderate pressures (0.1–1 mbar) [11]. Operating at such lower pressures significantly reduces the consumption of precursors which represent a major cost factor in CVD processes [12]. PECVD is widely used in the industrial fabrication of silicon-based materials, particularly for solar cell production [13–15]. Remote plasma chemical vapor deposition (RP-CVD), a subset of PECVD, distinguishes itself by positioning the plasma source away from the substrate, thereby avoiding ion bombardment effects [16–18]. This process has been studied for the growth of GaN, but much less as far as GaAs is concerned, with the most

* Corresponding author. Institut Photovoltaïque d'Ile-de-France (IPVF), 18 Boulevard Thomas Gobert, 91120, Palaiseau, France.

E-mail address: pere.roca@polytechnique.edu (P.R. Cabarrocas).

<https://doi.org/10.1016/j.mssp.2024.109069>

Received 20 August 2024; Received in revised form 25 October 2024; Accepted 30 October 2024

Available online 2 November 2024

1369-8001/© 2024 The Authors. Published by Elsevier Ltd. This is an open access article under the CC BY license (<http://creativecommons.org/licenses/by/4.0/>).

notable work being by A.D. Huelsman in the 1980s [19–21].

The ability to produce high quality GaAs thin films is essential to ensure the efficiency of the resulting solar cells, as the performance of electronic devices is highly dependent on the crystalline quality and uniformity of the layers [22]. In this study, we present the growth of high-quality homoepitaxial GaAs thin films using remote plasma CVD, allowing for reduced precursor consumption (only a few sccm vs. tens of L/min for MOCVD [23]) by operating at low pressure (0.5 mbar). We demonstrate the potential of this technique for the economical production of GaAs thin films for PV applications.

The remote plasma CVD reactor used in this study was described in a previous study dedicated to the growth of gallium nitride (GaN) on silicon substrates [24]. Here, depositions were performed on 4-inch (100) GaAs substrates, doped with Si ($\rho \approx 0.02 \text{ Ohm.cm}$). A hydrogen plasma treatment was applied to the GaAs substrate to remove oxygen and organic contaminants from its surface. Subsequently, an arsine plasma was performed for a few minutes to saturate the surface with As atoms. The deposition process is then initiated by introducing trimethylgallium diluted in hydrogen (H_2). The GaAs layer is grown at 500°C and 0.5 mbar.

To analyze the crystal structure of the films we used transmission electron microscopy (TEM). A thin lamella of the sample was prepared using a focused ion beam technique (dual-beam ThermoFisher SCIOS microscope). The TEM investigation was conducted using a FEI ThermoFisher Scientific Titan-Themis G3 electron microscope, operating at an acceleration voltage of 300 kV. This microscope is equipped with a CMOS (Ceta 16M) and a direct detection camera (Falcon-2) for both TEM and high-resolution TEM (HRTEM) imaging modes. Additional analyses of the structure were achieved by selected-area electron diffraction (SAED) using a small aperture of $10 \mu\text{m}$ and a camera length of 37 cm. Further structural investigations were performed by X-ray diffraction (XRD) with a Panalytical X'pert Pro diffractometer for out-of-plane ω - 2θ scans and a Rigaku SmartLab diffractometer equipped with a rotating anode for in-plane and pole-figure measurements. To gain

information on the morphological and topographical features of the films, we used a Scanning Electron Microscope (SEM) – Merlin Compact from Zeiss and an Atomic Force Microscope (AFM) PicoScan 3000 (resolution in XY: 1 nm, Z < 1 nm) from Agilent, respectively. The chemical composition was obtained by X-ray photoelectron spectroscopy (XPS) using a Thermo Scientific K-Alpha + spectrometer equipped with a monochromatic Al-K α x-ray source for excitation at 1486.6 eV and using an X-ray spot size of $400 \mu\text{m}$. Calibration of the spectrometer was done using Cu and Au samples following the ASTM-E-902-94 protocol. In complement to these surface analyses, depth-profiling was carried out using a monoatomic ion gun (Ar^+) with an energy of 1000 eV, at a current of 10 mA, and an ion gun orientation of 30° from the sample surface normal. The Thermo Scientific™ Avantage software was used for the XPS data treatment. Quantification was achieved with a Shirley background subtraction and RSF from the constructor library. To characterize the electronic properties, we first used a Jobin Yvon Horiba LabRAM HR Raman system to perform photoluminescence (PL) measurements at room temperature using 532 nm green laser excitation, a Synapse camera, a CCD detector and a grating with 1800 gr/mm. The laser was focused on the sample surface to a spot diameter of around $2 \mu\text{m}$ with an Olympus $10\times$ microscope objective. The Electrochemical Capacitance-Voltage (ECV) technique was used to obtain dopant profiles using a Wafer Profiler CVP21 from WEP Control. Finally, Hall effect measurements at room temperature were performed to determine the doping level and carrier mobility with the AMP55T system from Ecopia, under a magnetic field intensity of $B = 0.56 \text{ T}$, and a current of 1 mA. To perform the measurement, indium contacts were deposited at the four corners of a $1 \text{ cm} \times 1 \text{ cm}$ square sample.

The structure of the deposited GaAs film was first investigated by XRD analysis. The symmetrical 2Theta-Omega curve obtained for the sample is presented in Fig. 1 a), where only the 002 and 004 diffraction peaks are visible, revealing that the layer has the same crystalline structure and orientation as the substrate. The inset of Fig. 1 a) shows the HRXRD rocking curve of the 004 diffraction peak that exhibits a full

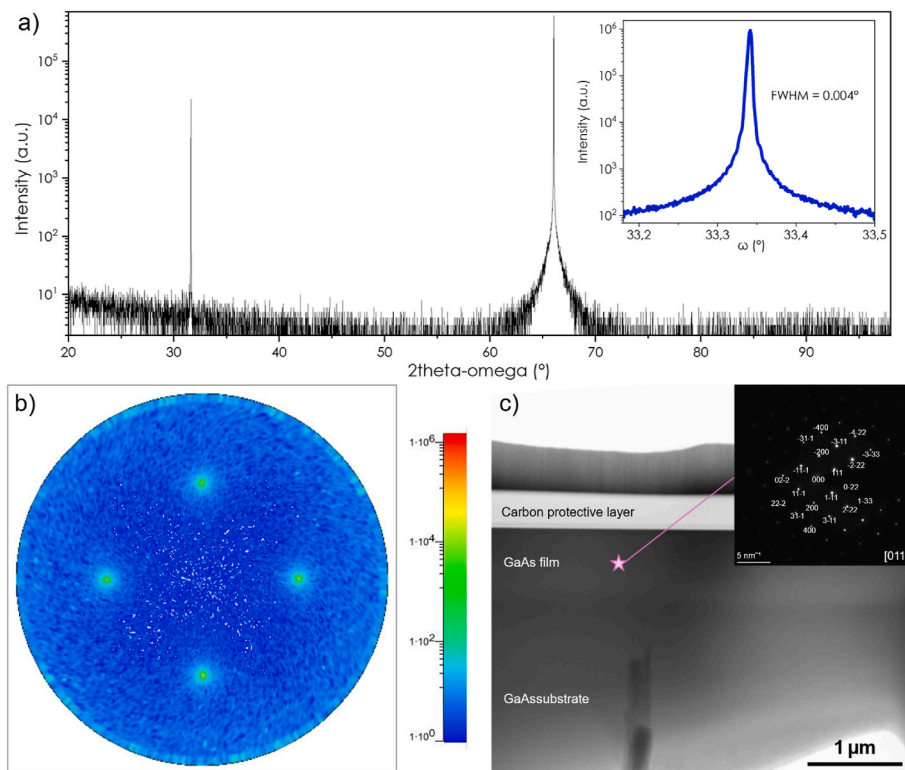


Fig. 1. a) XRD 2theta-omega scan with HRXRD rocking curve of 004 peak at $\phi = 0^\circ$ in inset, b) 111 in-plane pole figure and c) BF-STEM image with SAED pattern in inset of homoepitaxial GaAs grown by RP-CVD.

width at half maximum (FWHM) of 0.00446° , which indicates a very high film quality. In fact, with the instrumental configuration used, a monocrystalline 100 GaAs wafer has a FWHM of around 0.004° . Therefore, the structural quality of the GaAs film grown by RP-CVD is almost as high as that of a commercial GaAs substrate. A pole figure of the same sample is presented in Fig. 1 b), and displays a distinct and sharp spot pattern. The four spots correspond to the $\{111\}$ planes inclined at 54.7° to the 001 surface. The clarity and singularity of these spots on the pole figure indicate that the GaAs layer grown by RP-CVD exhibits a degree of twinning below the detection limit for this setup, indistinguishable of that of a wafer. TEM analyses were then carried out to corroborate these results. Fig. 1 c) presents a bright field (BF) STEM image of the lamella, showing no apparent dislocations. The interface between the substrate and the layer is not clearly discernible, confirming the quality of the epitaxy, and suggesting that the plasma cleaning treatment of the substrate is beneficial for the growth. Additional analyses of the structure were performed by selected-area electron diffraction (SAED) using a small aperture of $10\ \mu\text{m}$ and a camera length of 37 cm. The diffraction pattern of the epitaxial layer shown in the inset of Fig. 1 c) exhibits distinct spots, confirming the epitaxial growth and excellent crystalline quality of the grown GaAs layer. These spots correspond to the reflections from the set of 111 (0.326 nm) and 200 (0.286 nm) planes, observed along the $[011]$ zone-axis.

In terms of morphology, Fig. 2 a) shows a cross-sectional SEM image of the GaAs film grown on a GaAs substrate. The layer appears to be continuous without columnar features, only traces of mechanical cleavage from sample preparation are visible, and the interface with the substrate is sharp. The grown GaAs can be distinguished from the substrate due to the difference between its doping level and that of the substrate (see Fig. 4), to which secondary electron emission is sensitive [25,26]. Indeed, while it is very challenging to distinguish the interface using TEM, confirming the excellent quality of the homoepitaxy, this becomes possible with SEM using this doping contrast technique. Additionally, Fig. 2 a) indicates that the film grown in 1 h has a thickness of $2.9\ \mu\text{m}$, corresponding to a growth rate of approximately $3\ \mu\text{m}/\text{h}$, which is comparable to that achieved by MOCVD for GaAs [27]. As can be seen in Fig. 2 a), the layer appears to be very flat. To confirm and quantify this, we analyzed the top surface roughness using AFM, as shown in Fig. 2 b). We measured a root mean square (RMS) roughness of $0.2\ \text{nm}$, a value comparable to that of a commercial, polished GaAs wafer.

The depth-profiled composition of the layer obtained using XPS is presented in Fig. 3 a) for a total sputtering duration of 1000 s (substrate not reached). We observe surface contamination by carbon and oxygen, which is expected as the sample was exposed to air during transport from the growth reactor to the XPS instrument. Adventitious contamination and surface native oxide are removed after the first sputtering step, as demonstrated by the disappearance of the carbon- and oxygen-related peaks (C 1s, O 1s, Ga-O, As-O) in the spectra presented in Fig. 3 b-e). A III/V ratio of As/Ga = 1.005 ± 0.005 over the entire probed depth,

indicating that an homogeneous stoichiometry is achieved, and as expected given the high crystalline quality of the layers previously highlighted. The highly sensitive O-KLL Auger transition was also recorded, attesting that any O incorporated inside the layer is below the detection limit of the technique (0.01 at.%).

Fig. 4 a) shows the photoluminescence spectra with normalized intensities of the GaAs film produced by RP-CVD and of a GaAs wafer n-doped with Si ($\sim 1.10^{18}\ \text{cm}^{-3}$). Bare RP-CVD grown GaAs, i.e. without any passivation, shows a sharp PL peak (FWHM $\sim 55\ \text{meV}$ vs. $89\ \text{meV}$ for the wafer) indicating good crystalline quality and low defect density, in line with the previous structural results. The sample and the reference wafer exhibit a strong PL peak around the same photon energy ($\sim 1.4\ \text{eV}$), corresponding to the theoretical bandgap energy of GaAs. However, there is a slight shift towards low energies for GaAs layer grown by RP-CVD (peak position at $1.42\ \text{eV}$) compared to the GaAs n-type wafer (peak position at $1.44\ \text{eV}$), which suggests a p-type doping [28]. We analyzed the layers using ECV and Hall effect measurements to confirm our doping hypothesis and determine its level. Fig. 4 b) illustrates the results of the ECV analysis, showing the doping level and type as a function of etch depth within the layer. Two distinct regions are evident: a green region corresponding to the GaAs layer produced by RP-CVD, and a purple region corresponding to the substrate. The RP-CVD GaAs layer is identified as p-type, consistent with photoluminescence analysis, and exhibits uniform doping throughout its thickness at a value of approximately $1.04 \times 10^{18}\ \text{cm}^{-3}$. This doping arises from carbon present in the decomposition products of the organometallic gallium precursor, trimethylgallium. Hall effect measurements provided a comparable doping level value ($\sim 1.10^{18}\ \text{cm}^{-3}$), and also give a value of the hole mobility within the layer of $172\ \text{cm}^2\ \text{V}^{-1}\cdot\text{s}^{-1}$, consistent with what is expected for such a level of doping [29]. Using the same technique, the wafer is confirmed to be n-type with a doping level consistent with supplier specifications ($\sim 1.10^{18}\ \text{cm}^{-3}$).

In conclusion, our study successfully demonstrated the homoepitaxial growth of GaAs thin films at $3\ \mu\text{m}/\text{h}$ in a low-pressure RP-CVD reactor. Operating at $0.5\ \text{mbar}$ and 500°C , this approach leverages RF plasma to decompose the AsH_3 far from the substrate, while TMGa is directly introduced into the growth chamber and dissociated on the heated substrate. The resulting films exhibit remarkable characteristics comparable to commercial GaAs wafers, including excellent crystalline quality, as evidenced by SAED patterns and a 004 peak rocking curve FWHM of 0.004° , along with a surface roughness of $0.2\ \text{nm}$ as determined by AFM. Chemical analysis via XPS confirms a homogeneous composition throughout the film depth with a constant stoichiometry of 1/1 for As and Ga, and no traces of oxygen or carbon contamination being detectable. Furthermore, the samples display favorable optoelectronic properties, featuring a sharp photoluminescence peak (FWHM of $55\ \text{meV}$), a p-type doping concentration of $1.10^{18}\ \text{cm}^{-3}$, and a high mobility of $172\ \text{cm}^2\ \text{V}^{-1}\cdot\text{s}^{-1}$. Currently, the doping level is too high for our layers to be suitable as a base in a solar cell. Lowering this doping is feasible by using an alternative organometallic gallium precursor,

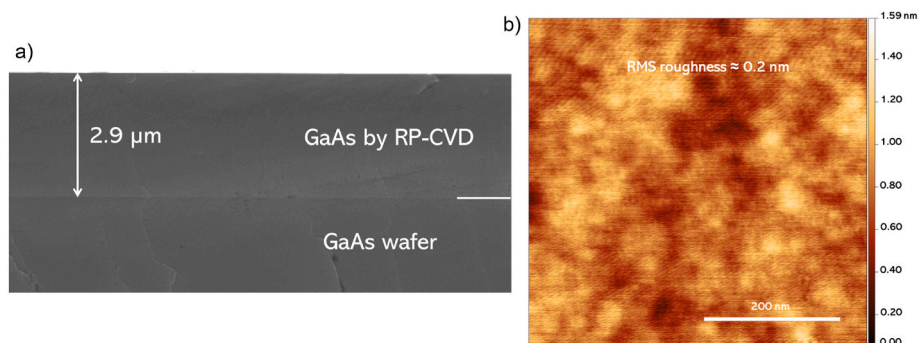


Fig. 2. a) SEM cross section image and b) AFM surface image of homoepitaxial GaAs grown by RP-CVD.

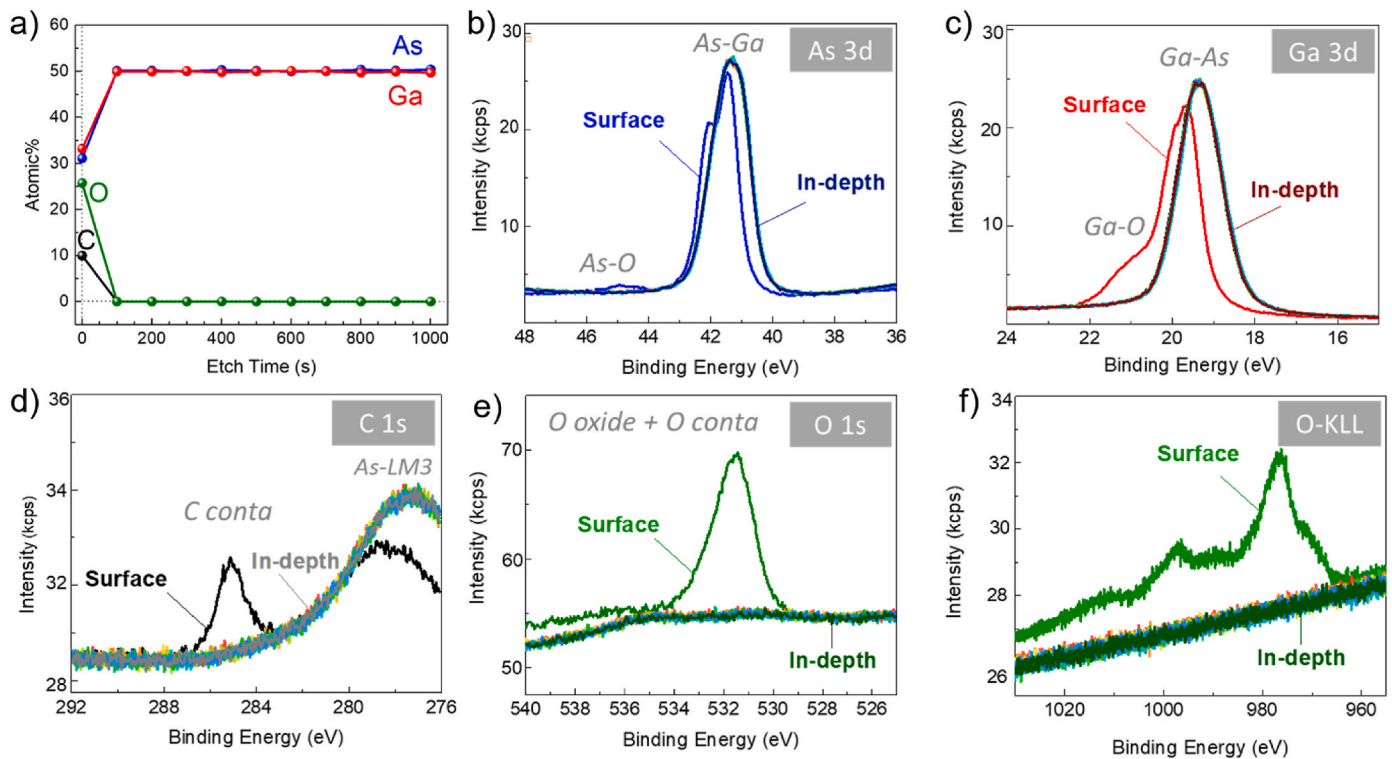


Fig. 3. a) In-depth profile of As, Ga, C and O from the surface to the bulk of the GaAs layer grown by RP-CVD and corresponding high energy resolution spectra of b) As 3d, c) Ga 3d, d) C 1s, e) O 1s photoemissions and f) O-KLL transition. Note that after the first etching, the peak overlap, shape, and intensity remain the same, which is an indication that the composition and chemistry are remarkably constant throughout the layer. The stoichiometry was calculated by averaging 10 analysis points within 100–1000 s etch time.

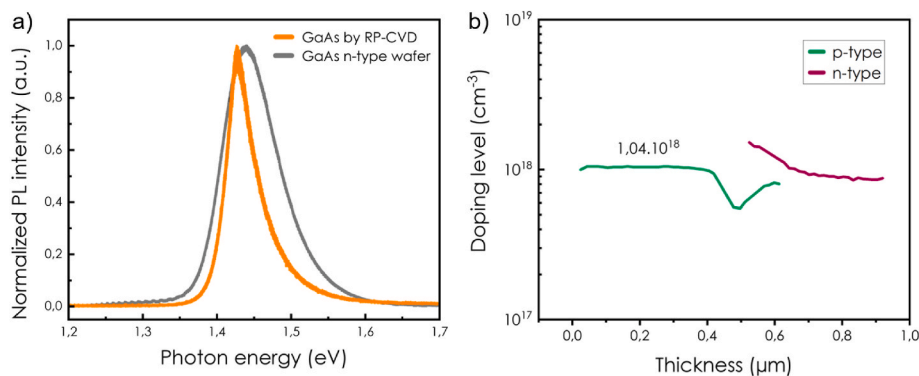


Fig. 4. a) Photoluminescence spectra and b) ECV profile of homoepitaxial GaAs grown by RP-CVD on a n-type GaAs wafer. Note that the ECV measurement is taken from a thinner sample.

TEGa, as demonstrated in several studies [30,31]. This approach will need to be validated in future work on our RP-CVD reactor. Nevertheless, these results demonstrate the potential of this technique for the economical production of GaAs-based devices, enabled by the RP-CVD process operating at low pressure and thus reducing gas consumption significantly compared to conventional methods such as MOCVD. It opens a new process window for the growth of device-grade GaAs thin films.

CRediT authorship contribution statement

Lise Watrin: Writing – review & editing, Writing – original draft, Visualization, Methodology, Investigation, Formal analysis, Data curation. **François Silva:** Writing – review & editing, Visualization, Validation, Conceptualization. **Ludovic Largeau:** Writing – review &

editing, Investigation, Formal analysis. **Nathaniel Findling:** Investigation, Formal analysis. **Mirella Al Katrib:** Writing – review & editing, Investigation, Formal analysis. **Muriel Boutemy:** Writing – review & editing, Investigation, Formal analysis. **Kassiogé Dembélé:** Writing – review & editing, Investigation, Formal analysis. **Nicolas Vaissière:** Writing – review & editing, Investigation, Formal analysis. **Cyril Jadaud:** Resources, Conceptualization. **Pavel Bulkin:** Writing – review & editing, Visualization, Resources. **Jean-Charles Vanel:** Software, Resources. **Erik V. Johnson:** Visualization, Supervision, Conceptualization. **Pere Roca i Cabarrocas:** Writing – review & editing, Visualization, Validation, Supervision, Methodology, Conceptualization.

Data availability statement

The data that supports the findings of this study are available within the article.

Declaration of competing interest

The authors declare that they have no known competing financial interests or personal relationships that could have appeared to influence the work reported in this paper.

Acknowledgments

We acknowledge the French national network RENATECH for funding the structural characterization (XRD and FIB for TEM). This project has been supported by the French Government in the frame of the program of investment for the future (Programme d'Investissement d'Avenir - ANR-IEED-002-01). The authors would like to thank Alexandre Blaizot for the AFM analysis made at IVPF.

Data availability

Data will be made available on request.

References

- [1] M.E. Levinshstein, S.L. Rumyantsev, M.S. Shur, *Properties of Advanced Semiconductor Materials: GaN, AlN, InN, BN, SiC, SiGe*, John Wiley & Sons, 2001.
- [2] M.E. Levinshstein, S.L. Rumyantsev, *GALLIUM ARSENIDE (GaAs)*, in: *Handbook Series on Semiconductor Parameters*, WORLD SCIENTIFIC, 1996, pp. 77–103.
- [3] M.-H. Chang, D. Das, P.V. Varde, M. Pecht, *Light emitting diodes reliability review*, *Microelectron. Reliab.* 52 (5) (2012) 762–782.
- [4] N.A. Aadit, S. Kirtania, F. Afrin, M. Alam, Q.D.M. Khosru, *High Electron Mobility Transistors: Performance Analysis, Research Trend and Applications*, 2017.
- [5] N. Papež, R. Dallaev, Ş. Tãlu, J. Kaštyl, *Overview of the current state of gallium arsenide-based solar cells*, *Materials* 14 (11) (2021) 3075.
- [6] M. Yamaguchi, *High-Efficiency GaAs-Based Solar Cells*, 2020.
- [7] M.A. Green, E.D. Dunlop, M. Yoshita, N. Kopidakis, K. Bothe, G. Siefert, X. Hao, *Solar cell efficiency tables (version 62)*, *Prog. Photovoltaics Res. Appl.* 31 (7) (2023) 651–663.
- [8] E.A. Alsema, R.F.A. Cuelenaere, W.C. Turkenburg, *Cost perspectives of GaAs thin-film solar cells*, in: A. Luque, G. Sala, W. Palz, G. Dos Santos, P. Helm (Eds.), *Tenth E.C. Photovoltaic Solar Energy Conference*, Springer Netherlands, Dordrecht, 1991, pp. 563–566.
- [9] S.P. Tobin, S.M. Vernon, C. Bajgar, S. Wojtczuk, M.R. Melloch, A. Keshavarzi, T. B. Stellwag, S. Venkatensan, M. Lundstrom, K.A. Emery, *Assessment of MOCVD- and MBE-growth GaAs for high-efficiency solar cell applications*, *IEEE Trans. Electron. Dev.* 37 (2) (1990) 469–477.
- [10] R. Pelzel, *A Comparison of MOVPE and MBE Growth Technologies for III-V Epitaxial Structures*, 2013.
- [11] H. Randhawa, *Review of plasma-assisted deposition processes*, *Thin Solid Films* 196 (2) (1991) 329–349.
- [12] K.A. Horowitz, T.W. Remo, B. Smith, A.J. Ptak, *A Techno-Economic Analysis and Cost Reduction Roadmap for III-V Solar Cells*, 2018.
- [13] P. Roca i Cabarrocas, *Plasma enhanced chemical vapor deposition of amorphous, polymorphous and microcrystalline silicon films*, *J. Non-Cryst. Solids* 266–269 (2000) 31–37.
- [14] K. Ouaras, S. Filonovich, B. Bruneau, J. Wang, M. Ghosh, E. Johnson, *Maskless interdigitated a-Si:H PECVD process on full M0 c-Si wafer: homogeneity and passivation assessment*, *Sol. Energy Mater. Sol. Cell.* 246 (2022) 111927.
- [15] Z. Sun, X. Chen, Y. He, J. Li, J. Wang, H. Yan, Y. Zhang, *Toward efficiency limits of crystalline silicon solar cells: recent progress in high-efficiency silicon heterojunction solar cells*, *Adv. Energy Mater.* 12 (23) (2022) 2200015.
- [16] C. Martin, K.S.A. Butcher, M. Wintrebert-Fouquet, A. Fernandes, T. Dabbs, P.P.-T. Chen, R. Carmen, in: H. Morkoç, C.W. Litton, J.-I. Chyi, Y. Nanishi, E. Yoon (Eds.), *Modeling and Experimental Analysis of RPCVD Based Nitride Film Growth*, 2008 689407. San Jose, CA.
- [17] G. Bruno, P. Capezzuto, M. Losurdo, *Growth of InP in a novel remote-plasma MOCVD apparatus : an approach to improve process and material properties*, *J. Phys. IV France* 5 (C5) (1995). C5-481-C5-488.
- [18] S. Barik, D. Liu, J.D. Brown, M. Wintrebert-Fouquet, A.J. Fernandes, P.P.-T. Chen, Q. Gao, V. Chan, I. Mann, *Remote plasma chemical vapour deposition of group III-nitride tunnel junctions for LED applications*, in: *Light-Emitting Devices, Materials, and Applications*, SPIE, 2019, pp. 181–188.
- [19] A.D. Huelsman, R. Reif, C.G. Fonstad, *Plasma-enhanced metalorganic chemical vapor deposition of GaAs*, *Appl. Phys. Lett.* 50 (4) (1987) 206–208.
- [20] A.D. Huelsman, L. Zien, R. Reif, *Plasma-controlled deposition of GaAs and GaAsP by metalorganic chemical vapor deposition*, *Appl. Phys. Lett.* 52 (9) (1988) 726–727.
- [21] A.D. Huelsman, R. Reif, *Characterization of a new reactor for remote plasma chemical vapor deposition*, *J. Vac. Sci. Technol. A* 7 (4) (1989) 2554–2561.
- [22] J. Li, A. Aierken, Y. Liu, Y. Zhuang, X. Yang, J.H. Mo, R.K. Fan, Q.Y. Chen, S. Y. Zhang, Y.M. Huang, Q. Zhang, *A brief review of high efficiency III-V solar cells for space application*, *Front. Physiol.* 8 (2021).
- [23] G. Brammertz, Y. Mols, S. Degroote, M. Leys, J. Van Steenberghe, G. Borghs, M. Caymax, *Selective epitaxial growth of GaAs on Ge by MOCVD*, *J. Cryst. Growth* 297 (1) (2006) 204–210.
- [24] L. Watrin, F. Silva, C. Jadaud, P. Bulkin, J.-C. Vanel, D. Muller, E.V. Johnson, K. Ouaras, P.R.I. Cabarrocas, *Direct growth of highly oriented GaN thin films on silicon by remote plasma CVD*, *J. Phys. D Appl. Phys.* 57 (31) (2024) 315106.
- [25] D.D. Perovic, M.R. Castell, A. Howie, C. Lavoie, T. Tiedje, J.S.W. Cole, *Field-emission SEM imaging of compositional and doping layer semiconductor superlattices*, *Ultramicroscopy* 58 (1) (1995) 104–113.
- [26] S.L. Elliott, R.F. Broom, C.J. Humphreys, *Dopant profiling with the scanning electron microscope—a study of Si*, *J. Appl. Phys.* 91 (11) (2002) 9116–9122.
- [27] G.B. Stringfellow, *Organometallic Vapor-phase Epitaxy: Theory and Practice*, Elsevier, 1999.
- [28] K. Ben Saddik, A.F. Braña, N. López, B.J. García, S. Fernández-Garrido, *Growth of silicon- and carbon-doped GaAs by chemical beam epitaxy using H2-diluted DTBSi and CBr4 precursors*, *J. Cryst. Growth* 571 (2021) 126242.
- [29] M. Sotoodeh, A.H. Khalid, A.A. Rezazadeh, *Empirical low-field mobility model for III-V compounds applicable in device simulation codes*, *J. Appl. Phys.* 87 (6) (2000) 2890–2900.
- [30] A.A. Aquino, T.S. Jones, *A comparative study of the adsorption and thermal decomposition of triethylgallium and trimethylgallium at GaAs(100) surfaces studied by electron energy loss spectroscopy*, *Appl. Surf. Sci.* 104–105 (1996) 304–311.
- [31] J.A. McCaulley, R.J. Shul, V.M. Donnelly, *Kinetics of thermal decomposition of triethylgallium, trimethylgallium, and trimethylindium adsorbed on GaAs(100)*, *J. Vac. Sci. Technol. A: Vacuum, Surfaces, and Films* 9 (6) (1991) 2872–2886.